Myotis rufoniger genome sequence and analyses: M. rufoniger's genomic feature and the decreasing effective population size of Myotis bats

Youngjune Bhak[1,2], Yeonsu Jeon[1,2], Sungwon Jeon[1,2], Oksung Chung[3,4], Sungwoong Jho[3], JeHoon Jun[3,4], Hak-Min Kim[1,2], Yongsoo Cho[1,2], Changhan Yoon[1,5], Seungwoo Lee[6], Jung-Hoon Kang[7], Jong-Deock Lim[7], Junghwa An[8], Yun Sung Cho[1,2,3]*, Doug-Young Ryu[6]*, Jong Bhak[1,2,3,4]*

1 The Genomics Institute, Ulsan National Institute of Science and Technology (UNIST), Ulsan, Republic of Korea, 2 Department of Biomedical Engineering, School of Life Sciences, Ulsan National Institute of Science and Technology (UNIST), Ulsan, Republic of Korea, 3 Personal Genomics Institute, Genome Research Foundation, Cheongju, Republic of Korea, 4 Geromics, Ulsan, Republic of Korea, 5 Department of Biomedical Science, School of Nano-Bioscience & chemical Engineering, Ulsan National Institute of Science and Technology (UNIST), Ulsan, Republic of Korea, 6 BK21 PLUS Program for Creative Veterinary Science Research, Research Institute for Veterinary Science, and College of Veterinary Medicine, Seoul National University, Seoul, Republic of Korea, 7 National Research Institute of Cultural Heritage, Cultural Heritage Administration, Daejeon, Republic of Korea, 8 Animal Resources Division, National Institute of Biological Resources, Incheon, Republic of Korea

* joys0406@gmail.com (YSC); dyryu@snu.ac.kr (DYR); jongbhak@genomics.org (JB)

Abstract

Myotis rufoniger is a vesper bat in the genus Myotis. Here we report the whole genome sequence and analyses of the M. rufoniger. We generated 124 Gb of short-read DNA sequences with an estimated genome size of 1.88 Gb at a sequencing depth of 66× fold. The sequences were aligned to M. brandtii bat reference genome at a mapping rate of 96.50% covering 95.71% coding sequence region at 10× coverage. The divergence time of Myotis bat family is estimated to be 11.5 million years, and the divergence time between M. rufoniger and its closest species M. davidii is estimated to be 10.4 million years. We found 1,239 function-altering M. rufoniger specific amino acid sequences from 929 genes compared to other Myotis bat and mammalian genomes. The functional enrichment test of the 929 genes detected amino acid changes in melanin associated DCT, SLC45A2, TYRP1, and OCA2 genes possibly responsible for the M. rufoniger's red fur color and a general coloration in Myotis. N6AMT1 gene, associated with arsenic resistance, showed a high degree of function alteration in M. rufoniger. We further confirmed that the M. rufoniger also has bat-specific sequences within FSHB, GHR, IGF1R, TP53, MDM2, SLC45A2, RGS7BP, RHO, OPN1SW, and CNGB3 genes that have already been published to be related to bat's reproduction, lifespan, flight, low vision, and echolocation. Additionally, our demographic history analysis found that the effective population size of Myotis clade has been consistently decreasing since ~30k years ago. M. rufoniger's effective population size was the lowest in Myotis bats, confirming its relatively low genetic diversity.

Introduction

M. rufoniger is a species of vesper bat in the family Vespertilionidae [1]. It can be distinguished from other bats by its rusty orange fur (S1 Picture) and is therefore called 'golden bat' or 'red bat' in South Korea (Republic of Korea). Recently, its scientific name has been re-assigned to *M. rufoniger* from *Myotis formosus tsuensis* based on a molecular phylogeny and morphological study of bats [2]. Although its population is not assessed systematically, it is apparently a rare species that has only been collected in a handful of localities [2]. In South Korea, *M. rufoniger* is protected and designated as a natural monument. Being one of the most well-known and iconic protected wild animals in South Korea, even an *M. rufoniger* exhibition center is also in operation (golden bat exhibition center in Hampyeong County, South Korea).

In 2012, a fruit bat *Pteropus alecto* and an insectivorous *Myotis davidii* genomes were published, reporting bat-specific amino acid sequences on *TP53* (Tumor Protein P53) and *MDM2* (MDM2 Proto-Oncogene) genes that are associated with DNA damage checkpoint and DNA repair pathways. They provided insights into bats' evolution of high metabolic rate and an increased amount of free radicals that are associated with flight [3]. In 2013, the Brandt's bat (*Myotis brandtii*) genome analysis further identified unique amino acid sequence changes in *GHR* (Growth Hormone Receptor), *IGF1R* (Insulin Like Growth Factor 1 Receptor), *FSHB* (Follicle Stimulating Hormone Beta Subunit), *SLC45A2* (Solute carrier family 45, member 2), *RGS7BP* (Regulator of G-protein signaling 7 binding protein), *RHO* (Rhodopsin), *OPN1SW* (Opsin 1 [Cone Pigments], Short-Wave-Sensitive), and *CNGB3* (cyclic nucleotide gated channel beta 3) genes, providing new insights into bats' delayed ovulation during hibernation, long lifespan, small body size, low vision, and echolocation [4].

As such, a set of close but distinct species genomes enable prediction of variants that may contain significant geno-phenotype association information [5–8]. This close species comparative genomics approach has been applied to *M. rufoniger* genome analyses to identify the species-specific variants that can confer functional and hence evolutionary adaptation of the *M. rufoniger*. To confirm and further identify such species-specific or bat-specific sequence changes, it is critical to evaluate such amino acid changes with as many genomes as possible at different levels of background comparison species. Thus, it is important to build biological resource with continuous sequencing of various species genomes.

A complete mitochondrial genome of *M. rufoniger* has been published already [9], while no whole-genome sequence has been reported yet, thus limiting the investigation of autosomal genetic signatures for environmental adaptations of *M. rufoniger*. Furthermore, the demographic history of a species can only be reconstructed accurately from deeply sequenced whole genomes [10,11]. Here, we provide a whole genome analysis of *M. rufoniger* by producing massively parallel short DNA sequences (approximately 124 Gb) with its genomic features and unique amino acid sequences, accompanied by its demographic history and genetic diversity.

Results

Whole genome sequences of *M. rufoniger*

The genomic DNA from the wild carcass of *M. rufoniger* found in Gosudonggul cave, Danyang, in South Korea, was sequenced using Illumina HiSeq2000 platform. A total of 124 Gb of paired-end short DNA sequences were produced with a read length of 100 bp, and target insert sizes of 566 bp and 574 bp from two genomic libraries. After reducing low sequencing quality reads and possible microbial contaminated reads, we acquired a total of 115 Gb of DNA sequences (Table 1; S1 Table). To confirm the species identification of the sample, a phylogenetic analysis was performed using a multiple sequence alignment of mitochondrial

Table 1. Sequencing and mapping statistics of *M. rufoniger* genome.

	Myotis bat references		
	M. brandtii	**M. davidii**	**M. lucifugus**
Sequenced reads		1,240,507,648	
Low quality filtered reads		1,152,154,630	
Contamination filtered reads		1,149,260,980	
Mapped reads	1,109,045,915	1,101,733,443	1,095,435,354
Mapping rate	96.50%	95.86%	95.32%
Deduplicated reads	1,023,540,144	1,017,982,320	1,010,388,456
Depth coverage	49.5 ×	51.5 ×	49.1 ×
1× genome coverage	90.17%	87.65%	92.29%
5× genome coverage	87.83%	85.68%	89.88%
8× genome coverage	86.47%	84.60%	88.52%
10× genome coverage	85.58%	83.88%	87.63%
1× CDS coverage	98.86%	99.10%	98.13%
5× CDS coverage	97.68%	98.19%	96.29%
8× CDS coverage	96.60%	97.33%	94.88%
10× CDS coverage	95.71%	96.60%	93.81%
The number of homozygous SNVs	50,615,560	56,635,858	50,441,069
The number of heterozygous SNVs	8,044,633	8,008,552	8,306,592
The number of homozygous indels	4,197,521	4,231,431	4,313,780
The number of heterozygous indels	517,253	457,868	512,018
The number of consensus genes	17,274	16,419	17,141
The number of consensus genes without gap	12,841	12,618	12,941

cytochrome b sequences, and our sample was verified to be the closest to *M. rufoniger* (S1 Fig). We performed a *K*-mer analysis (*K* = 17) using the *M. rufoniger* whole genome sequences, and its genome size was predicted to be approximately 1.88 Gb (S2 Fig; S2 Table). This is similar to those of other bat species and smaller than those of other mammals [3,4,12]. Since there is no *de novo* assembled *M. rufoniger* genome, the DNA reads were aligned to all three available *Myotis* bat reference genomes (*M. brandtii*, *M. davidii*, and *M. lucifugus*; Table 1; S3 Table). The consensus DNA sequences of *M. rufoniger* were generated by substituting *M. rufoniger* single nucleotide variants (SNVs) detected from the whole genome sequencing data against the three reference genomes. The genome coverage (≥10×, 87.63%) was the highest when the *M. lucifugus* assembly was the reference, while the coding sequence (CDS) coverage (≥10×, 96.60%) was the highest when the *M. davidii* genome was the reference. The number of SNVs (58,660,193) was the lowest when the *M. brandtii* was the reference, while the number of small insertions and deletions was the lowest when the *M. daividii* was the reference. However, when the *M. brandtii* assembly was the reference, the mapping rate (96.50%) and the number of consensus genes (17,247) was the highest. Therefore, we used *M. brandtii* reference-guided *M. rufoniger* consensus sequences for following analyses.

We examined the base composition of *M. rufoniger* genome (S4 Table) and found that the ratio of GC content was higher in the CDS region (52.15 ~ 52.95%) than that of the whole genome (41.49 ~ 42.28%), and this is concordant with the other mammalian species (the GC content ratios of the other species were 48.98 ~ 54.35% in the CDS region and 37.82 ~ 42.93% in the whole genome; S5 Table). The proportion of known transposon-derived repeats in the *M. rufoniger* genome was 19.05%, which is comparable with those of other bats (19.34 ~

33.32%), but significantly lower than those of other mammalian genomes (25.27 ~ 51.62%; S6 Table).

The body of the *M. rufoniger* carcass used in this study was damaged and its morphological sex determination was not possible. We therefore compared its heterozygosity in X-chromosomal scaffolds with that of the other male *Myotis* bat (S7 Table). Since mammalian males have both X and Y sex chromosomes while females have two X chromosomes, a male individual has to show a lower heterozygosity in X chromosome than that of a female individual. Our sample showed an even lower heterozygosity in X-chromosomal scaffolds than that of the male *M. davidii* individual, indicating that it is clearly a male.

## Relationship of *M. rufoniger* to other mammalian species

We identified orthologous gene clusters from 13 mammalian genomes (seven bat genomes: *Myotis brandtii*, *Myotis lucifugus*, *Myotis davidii*, *Eptesicus fuscus*, *Pteropus alecto*, *Pteropus vampyrus*, and *Rousettus aegyptiacus*, and six other mammalian genomes: *Homo sapiens*, *Mus musculus*, *Bos taurus*, *Equus caballus*, *Heterocephalus glaber*, and *Monodelphis domestica*; S2 Table) using OrthoMCL software [13]. The *M. rufoniger* genes were matched and added to the orthologous clusters of *M. brandtii*'s genes, and 6,782 single-copy gene families among the 14 species were identified [7].

The divergence times of *M. rufoniger* and the 13 mammals were estimated using 1,258,141 four-fold degenerate sites from the 6,782 single-copy genes (Fig 1). The closest clade to bats was *E. caballus* (horse) and *B. taurus* (cow) clade (diverged at 79.45 million years ago [MYA]). The *Myotis* bats diverged into its current clade approximately 11.52 MYA. *M. davidii* was estimated to be the closest to the *M. rufoniger* among the three *Myotis* bats used in this study. The divergence time between *M. rufoniger* and *M. davidii* was estimated to be 10.41 million years, indicating a fairly recent divergence which is suitable for our close species comparative genomics analyses.

M. rufoniger specific amino acid sequences

From previous studies [3,4], bat-specific amino acid sequences within *FSHB*, *GHR*, *IGF1R*, *TP53*, *MDM2*, *SLC45A2*, *RGS7BP*, *RHO*, *OPN1SW*, and *CNGB3* genes were reported. They represent some general characteristics of *Myotis* bats: delayed ovulation (*FHSB*), long lifespan (*GHR* and *IGF1R*), powered flight (*TP53* and *MDM2*), echolocation (*SLC45A2* and *RGS7B*), and low vision (*RHO*, *OPN1SW*, and *CNGB3*). The same amino acid sequences within the above listed genes were also identified in the *M. rufoniger* genome (S3 Fig).

To further identify bat-specific amino acid sequences linked to environmental adaptations and unique evolutionary features, we investigated *M. rufoniger* specific amino acid changes compared to other *Myotis* bats. A total of 3,366 unique amino acid changes (uAACs) from 2,125 genes were identified in *M. rufoniger*. Among them, 1,696 uAACs from 1,228 genes were predicted to be function altering by the protein variation effect analyzer (PROVEAN) software (variant score ≤ -2.5; S8 Table) [14]. These function-altering variants and associated genes can provide insights onto *M. rufoniger* specific evolutionary adaptation. When gap-containing genes were excluded, 1,239 uAACs from 929 genes were predicted to be function altering (S9 Table). A functional enrichment analysis of the 929 genes having function-altering uAACs was performed using DAVID (Database for Annotation Visualization and Integrated Discovery) tool [15]. The probably function-altered genes were significantly enriched in reproduction related terms (Gene Ontology [GO] analysis with a P–value ≤ 0.05 by EASE scores [modified Fisher's exact test] and with a 10% of false discovery rate [FDR]) including reproductive processes in a multicellular organism (P-value: 0.00026, 39 genes, GO: 0048609), ovulation cycle
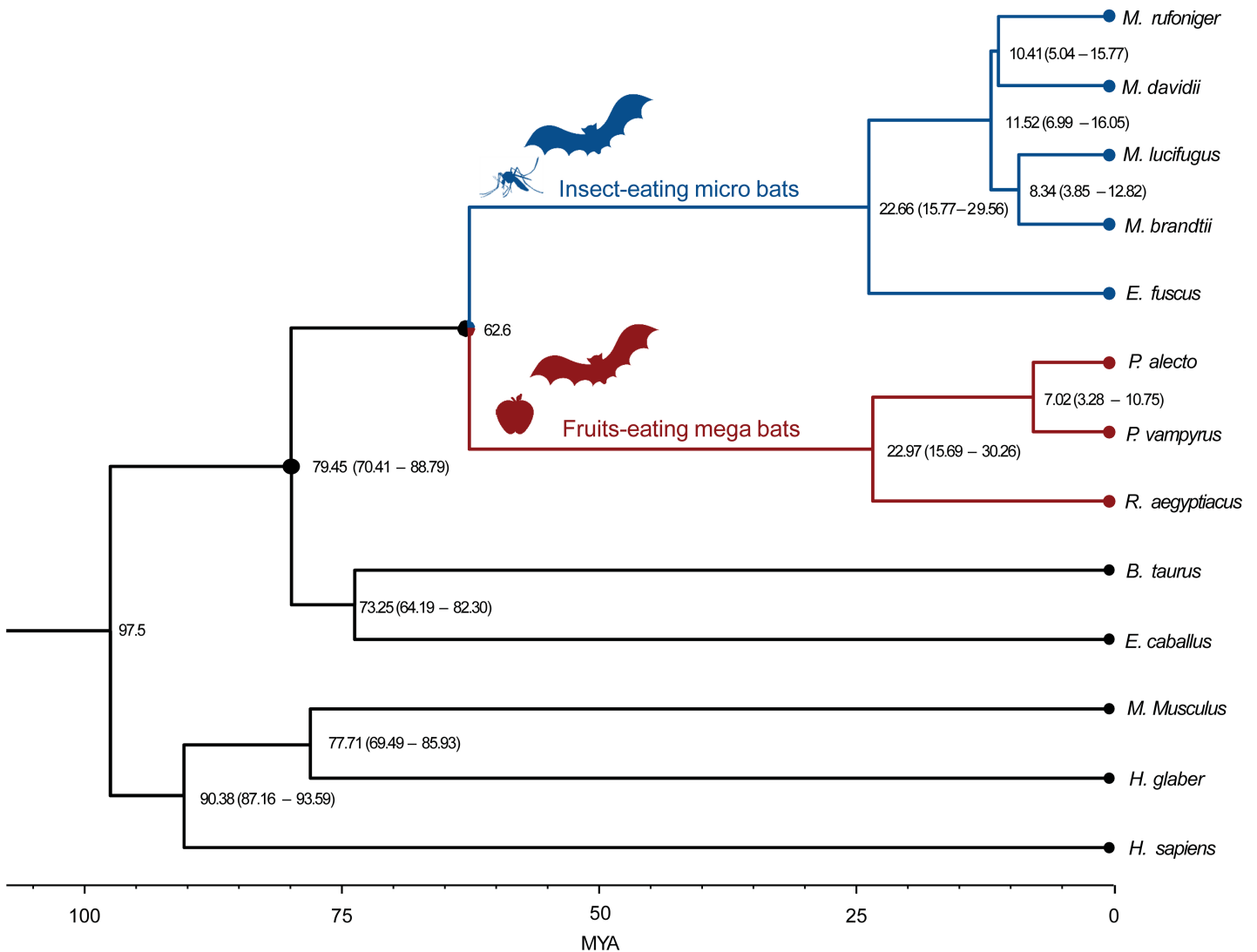
Fig 1. Phylogenetic relationships and divergence times in bats and mammalian species. The estimated divergence time (million years ago; MYA) is given at the nodes, with the 95% confidence intervals in parentheses. The calibration times of *M. brandtii—H. sapiens* (97.5 MYA), and *M. brandtii—P. alecto* (62.6 MYA) were derived from the TimeTree database. Colored branches and circles represent bat groups (*blue*: insect-eating microbat, *red*: fruits-eating mega bat). *M. domestica*, used as an outgroup species, was excluded in this figure.

(*P*-value: 0.00052, 11 genes, GO: 0042698), and gamete generation (*P*-value: 0.0017, 31 genes, GO: 0007276; S10 Table). In *M. rufoniger*, pigment related terms were significantly enriched in the function-altered genes as in the melanin biosynthetic process (*P*-value: 0.0037, 4 genes, GO: 0042438; S10 Table). The genes are *DCT* (Dopachrome tautomerase), *SLC45A2* (Solute carrier family 45), *TYRP1* (Tyrosinase-related protein 1), and *OCA2* (Oculocutaneous albinism II). We could identify some uAACs in *DCT*, *SLC45A2*, *TYRP1*, and *OCA2* genes in the other *Myotis* bats as function-altering using PROVEAN software (Table 2; S11 Table) [14] indicating those genes are not only specific to *M. rufoniger*'s red fur color. The multiple sequence alignments and specific amino acid sequences are presented in S4 Fig.

Table 2. *Myotis* bats' uAACs within melanin associated genes.

Gene	Description	The number of uAACs (The number of uAACs with PROVEAN score $\leq$ -2.5)			
		M. rufoniger	*M. brandtii*	*M. davidii*	*M. lucifugus*
DCT	Dopachrome tautomerase	2 (2)	0 (0)	0 (0)	1 (0)
SLC45A2	Solute carrier family 45	3 (1)	0 (0)	0 (0)	0 (0)
TYRP1	Tyrosinase-related protein 1	2 (1)	0 (0)	1 (1)	0 (0)
OCA2	Oculocutaneous albinism II	3 (3)	1 (0)	0 (0)	2 (2)

As we were interested in the variants' whole gene function, all the PROVEAN variant scores of each gene were summed up. We then ranked the sums of the function-altered gene candidates (S12 Table). For the top 20 genes, the same analysis was carried out in the other *Myotis* bat species for comparison (Table 3; S13 and S14 Tables). We ranked *M. rufoniger*'s genes according to the numbers of variants and summed variant scores, and compared them to those of other *Myotis* bat genes. From the result, *N6AMT1* (N-6 Adenine-Specific DNA Methyltransferase 1) showed the fourth-lowest sum of variants scores (sum of PROVEAN variant scores: -40.285 and number of variants: six *in M. rufoniger*; no uAAC in the other *Myotis* bats), indicating a high degree of function alteration of *N6AMT1* in *M. rufoniger*. The multiple sequence alignments and specific amino acid sequences are presented in S5 Fig.

Demographic history and the genetic diversity of *Myotis* bats

Deeply sequenced genomes allow the estimation of population structure history [10,11]. To investigate the demographic history of *Myotis* bats, a pairwise sequentially Markovian coalescent (PSMC) model inference analysis was conducted [11]. *M. rufoniger* was estimated as the most flourished species around 30 ~ 300 k years ago compared to the other *Myotis* bats, and its demographic history showed that its population peak was 50 k years ago (Fig 2). However, its effective population size was dramatically decreased during the last glacial period (10 ~ 50 k years ago), and it was estimated to be the lowest in present. Also, a consistent decline in the effective population size of *Myotis* bats since ~30 k years ago was found (Fig 2). We further investigated the genomic diversity (which can be affected by population size) of the *M. rufoniger* and compared it to those of the other *Myotis* bats. The *M. rufoniger* genetic diversity (0.00391), based on the heterozygous SNV rate, was lower than those of the *M. davidii* (0.00471) and the *M. brandtii* (0.00614), confirming the *M. rufoniger*'s low effective population size (S13 Table).

Discussion

The function-altering variants containing genes of the *M. rufoniger* were concentrated in reproduction associated pathways. Prolonged sperm storage is a common behavior in Vespertilionidae (including genus *Myotis*, *Pipistrellus*, *Nyctalus*, *Eptesicus*, *Vesoertilio*, *Chalinolobus*, and *Plecotus*) and Rhinolophidae family species [16–18], and thus it is probably not *M. rufoniger* specific as reproduction related genes are always under strong natural selection. Therefore, such hits can be regarded as general or even a kind of artefact. Therefore, further detailed functional verification is necessary to understand the roles of each uAAC in functional categories such as reproduction.

The previous bat studies reported unique variants representing some general characteristics of *Myotis* bats: delayed ovulation (*FHSB*), long lifespan (*GHR* and *IGF1R*), powered flight (*TP53* and *MDM2*), echolocation (*SLC45A2* and *RGS7B*), and low vision (*RHO*, *OPN1SW*, and *CNGB3*) [3, 4]. We confirmed the reported amino acid sequences within the above listed genes

**Table 3. The summed PROVEAN variant score for top 20 ranked genes. The lower the more significant.**

Gene	Description	Sum of the PROVEAN variant scores	
		M. rufoniger	Other *Myotis* bats
BCO1	Beta-Carotene Oxygenase 1	-51.29	-8.13 ~ 0
CCDC184	Coiled-coil Domain Containing 184	-47.77	-2.88 ~ 0
PCM1	Pericentriolar material 1 protein	-40.61	-19.04 ~ 0
N6AMT1	N-6 adenine-specific DNA methyltransferase 1	-40.29	0 ~ 0
MDN1	Midasin AAA ATPase 1	-37.90	-32.07 ~ -5.80
CEP350	Centrosomal protein 350	-37.30	-15.16 ~ -4.92
WNK2	WNK Lysine Deficient Protein Kinase 2	-34.67	-17.12 ~ -4.79
SPG11	Spastic Paraplegia 11	-29.39	-18.19 ~ 0
C10orf12	Uncharacterized protein	-29.01	-18.97 ~ 0
C1orf228	Uncharacterized protein	-28.71	-8.22 ~ 0
NOC2L	NOC2 Like Nucleolar Associated Transcriptional Repressor	-28.61	0 ~ 0
CPLX3	Complexin 3	-27.85	-7.67 ~ 0
KIAA1462	Junctional Protein Associated With Coronary Artery Disease	-27.73	-3.22 ~ 0
ALPK2	Alpha Kinase 2	-26.00	-9.09 ~ 0
PTRH1	peptidyl-tRNA hydrolase 1	-25.30	0 ~ 0
MYO16	Myosin XVI	-24.71	-14.57 ~ 0
KIAA0922	Transmembrane protein 131-like	-24.59	-4.33 ~ 0
OAT	Ornithine aminotransferase	-24.44	-11.60 ~ 0
SPAG17	sperm associated antigen 17	-23.71	-16.24 ~ -2.18
IPMK	Inositol Polyphosphate Multikinase	-23.47	0 ~ 0

https://doi.org/10.1371/journal.pone.0180418.t003

were conserved in the *M. rufoniger* as in other bat genomes (S3 Fig), supporting that those variants are *Myotis* bat-wide not one species-specific nor individual-specific variants.

We also found that the function-altering unique variants containing the genes of the *M. rufoniger* were concentrated in a melanin associated pathway including *DCT*, *SLC45A2*, *TYRP1*, and *OCA2* genes. *TYRP1* and *DCT* genes are known to influence the quantity and quality of melanin [19]. Mutations on the *TYRP1* gene are known to be associated with "rufous/red albinism", causing reddish-brown skin or red hair [20–22]. The protein (melanocyte-specific transporter protein) encoded by *OCA2* gene has been reported as a transporter of tyrosine, the precursor to melanin synthesis [23]. Variants within the *SLC45A2* gene have shown association with hair color, affecting red/yellow pheomelanin pathway [24–25]. In this context, we suggest that the variants within the *DCT*, *SLC45A2*, *TYRP1*, and *OCA2* genes are likely responsible for the *M. rufoniger*'s rusty orange fur color, which distinguish it from the other bats. However, fewer but certain uAACs within the *DCT*, *SLC45A2*, *TYRP1*, and *OCA2* genes were also found in the other *Myotis* bats, suggesting a possible general role of those genes in bat-wide coloration. Therefore, a set of bat species with color diversity will be required for further analyses to understand the precise geno-phenotype associations in coloration.

In the *M. rufoniger* genome, *N6AMT1* gene showed a high degree of function alteration. The protein (HemK methyltransferase family member 2) encoded by *N6AMT1* gene can transform monomethylarsonous acid to dimethylarsinic acid, conferring resistance of mammalian cells to arsenic-induced toxicity [26]. An elemental analysis in the tissues from the *M. rufoniger* individual analyzed in the present study showed a very high concentration of arsenic in its intestinal tissue [27], suggesting that the *M. rufoniger* individual was exposed to food or water highly contaminated with arsenic. In this context, uAACs in *N6AMT1* can be considered as a possible chemical adaptation signature. It can be a generally stressful condition for the bats
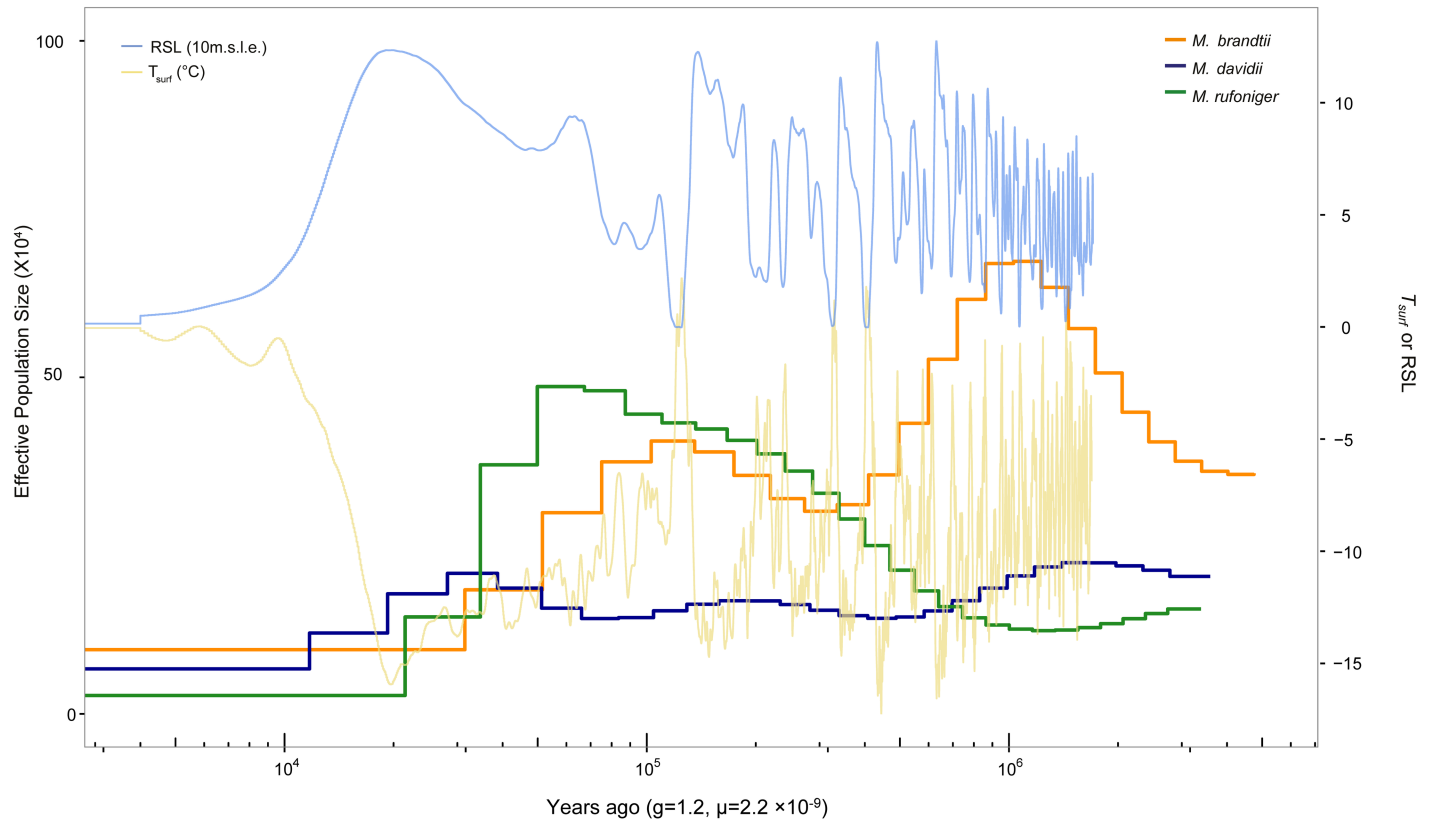
Fig 2. Demographic history of *Myotis* bats. T_{surf}, atmospheric surface air temperature (T indicates temperature, surf indicates surface); RSL, relative sea level; 10 m.s.l.e., 10 m sea level equivalent; g, generation time (years); μ, mutation rate per base pair per year.

living in caves, because caves are hazardous due to various harmful elements and chemicals such as heavy metals [28]. However, until a further experimental validation is carried out, it is a very speculative hypothesis of rapid adaptation to harmful cave elements. Furthermore, this study used genomic data from only one individual for each species and the variant comparison analysis can be biased by individual-specific variants. More genomes are necessary to be sequenced to confirm that our finding's general applicability in both *M. rufoniger* and *Myotis* bats.

The *M. rufoniger* showed the lowest effective population size compared to other *Myotis* bats from the PSMC analysis. This does not necessarily indicate that they are the most endangered as they are fairly widely spread. It is perhaps more reasonable to attribute it to very recent human encroachment. It is also shown that the population size of the *M. rufoniger* was dramatically decreased during the latter part of the last glacial period. There was a consistent decline of *Myotis* bat family's effective population size since ~30 k years ago. However, we cannot determine whether it is a bat-wide or *Myotis* bat specific phenomenon either, because we conducted the PSMC analysis using a small number of species. The dramatic decrease in the

population size of the *M. rufoniger* could be a Korean *M. rufoniger* specific phenomenon. Therefore, a set of diverse species will be required to accurately model the bats' effective population size history.

In conclusion, we report the first whole genome sequences of the *M. rufoniger* with bioinformatics analyses such as multiple sequence alignment, function altering uAAC prediction, functional enrichment, and population size estimation using PSMC. These provided us with some speculative insights on how bats adapted to environment sustaining the current behavioral, physiological, and demographic features such as bat's prolonged sperm storage during reproduction, long lifespan, powered flight, low vision, echolocation, possible arsenic resistance, fur coloration, and consistently decreasing effective population sizes in their demographic history.

Materials and method

Sample and genome sequencing

The partially decomposed carcass of *M. rufoniger* was found in August 2012 at Gosudonggul cave in Danyang, South Korea (coordinates: 36˚ 59' 18.67" N, 128˚ 22' 53.26" E; elevation: 180.65 m) by Gosudonggul cave management office staff. The *M. rufoniger* was moved to the Natural Heritage Center of the Cultural Heritage Administration (South Korea) and kept frozen (Keeping temperature: -70˚C). We acquired the *M. rufoniger* sample from the Natural Heritage Center under the Cultural Heritage Administration permit in June 2013. The wing membrane tissue, which seemed not decayed, was acquired for genomic DNA sequencing (S1 Picture).

Its genomic DNA was sequenced using Illumina HiSeq2000 platform, with a read length of 100 bp and insert sizes of 566 and 574 bp from two genomic libraries. The DNA was extracted using a Tiangen Micro DNA Kit. The amount of DNA was quantified by fluorometry using a UV spectrophotometer (Tecan F200). A partial DNA degradation was identified by electrophoresis (S2 Picture), but it was judged good resulting in no significant sequencing quality problems. The genomic DNA was sheared to approximately 566 bp and 574 bp using a Covaris S2 Ultrasonicator, and then used in the preparation of whole-genome shotgun libraries according to Illumina's library preparation protocols. The efficacy of each step of the library construction was ascertained using a 2100 Bioanalyzer (S6 Fig). The final dilutions of the two libraries were then sequenced using a HiSeq2000 sequencer with the TruSeq PE Cluster kit v3-cbot HS and TruSeq SBS kit v3-HS for 200 cycles.

Sequencing read filtering

A DNA read was filtered out when the read' Q20 base content was lower than 70%, using IlluQCPRLL.pl script of NGSQCToolkit (ver 2.3.3; S1 Table) [29]. We additionally downloaded genome data of the other bats (*Myotis brandtii*, *Myotis davidii*, *Myotis lucifugus*, *Pteropus Alecto*, and *Pteropus vampyrus*) from the NCBI database. Low quality DNA reads from the other bats were also filtered out using the same method (S1 Table). The possible microbial contaminated DNA reads were filtered out when the reads' alignment scores to microbial (bacteria and fungi) genomes were higher than that to the *Myotis* bat genomes (*M. brandtii*, *M. davidii*, and *M. lucifugus*; S3 Table). We used microbial genomes that were downloaded from Ensembl database and the three *Myotis* bat genome assemblies were from NCBI. The DNA reads were mapped to the microbial and *Myotis* bat genomes using BWA-MEM algorithm of BWA (version 0.7.15) with Mark shorter split hits as a secondary option (-M) [30]. The rmdup command of SAMtools (ver 0.1.19) was used to remove PCR duplicates [31]. The possible

microbial contaminated reads in the other *Myotis* bats were also filtered out by using the same method but mapping was to their own genome assemblies (S1 Table).

Species identification

To construct the phylogenetic tree and identify the sample's species, the mitochondrial cytochrome b consensus sequence was generated by mapping the sequencing data to the *M. rufoniger* mitochondrial cytochrome b sequence (GenBank accession number: HQ184048.1) using BWA-MEM algorithm of BWA (version 0.7.15) with Mark shorter split hits as a secondary option (–M) [30]. The reads were realigned using the GATK (version 2.5–2) RealignerTargetCreator and IndelRealigner algorithms to minimize the read alignment mismatches [32]. The rmdup command of SAMtools (ver 0.1.19) was used to remove PCR duplicates [31]. The variants from the whole genome sequencing data against the reference were called using mpileup command of SAMtools (version 0.1.19) with–E option to minimize the noise, -A option to use regardless of insert size constraint, -q 20 to consider only high quality mapping reads, and–Q 30 to consider only high quality bases [31]. The called variants were filtered using vcfutils.pl varFilter command of SAMtools (ver 0.1.19) with -d 8 option (minimal depth of 8) [31]. SNVs detected from the whole genome sequencing data against the reference were substituted to construct mitochondrial cytochrome b consensus sequence of the *M. rufoniger* using vcfutils.pl vcf2fq command of SAMtools (ver 0.1.19) with -l 5 option (no indel present within a 5 bp window) [31]. A multiple sequence alignment of the mitochondrial cytochrome b sequences was conducted using MUSCLE (version 3.8.31) program with default options [2,33]. A phylogenetic analysis was conducted using MEGA 7.0 program [34]. The phylogenetic tree was inferred by using a Maximum Likelihood method based on the Tamura-Nei model with 1,000 replicates bootstrapping [35,36]

Genome size estimation

For a *K*-mer analysis, KmerFreq_HA command of SOAPec program in SOAPdenovo2 package was used with a *K* = 17 option [37]. The genome size was estimated from the number of *K*-mers (depth > 3) divided by the peak depth of the *K*-mer graph.

Mapping sequence data

The filtered sequenced reads were mapped to the three *Myotis* bat genome assemblies (*M. brandtii*, *M. davidii*, and *M. lucifugus*) using BWA-MEM algorithm of BWA (version 0.7.15) with Mark shorter split hits as a secondary option (-M) [30]. The reads were realigned using the GATK (version 2.5–2) RealignerTargetCreator and IndelRealigner algorithms to minimize the read alignment mismatches [32]. The rmdup command of SAMtools (ver 0.1.19) was used to remove PCR duplicates [31]. The variants of *M. rufoniger* were called using mpileup command of SAMtools with–E, -q 20, -A, and–Q 30 options [31]. The called variants were filtered using vcfutils.pl varFilter command of SAMtools (ver 0.1.19) with -d 8 and -D 250 options (minimal depth of 8 and maximal depth of 250) [31]. The DNA consensus sequences of *M. rufoniger* were generated by substituting the *M. rufoniger* SNVs detected from the whole genome sequencing data to each reference bat genome using the vcfutils.pl vcf2fq command of SAMtools (ver 0.1.19) with -l 5 option [31].

Repeat annotation

RepeatMasker (version 4.0.5) was used to identify transposable elements by aligning the *M. rufoniger* consensus genome sequence against a library of *M. brandtii* with default option [38].

For the comparison of the *M. rufoniger*'s repeat annotation with the other species, the same method was used for other genome references.

Sex determination

Male *M. davidii* reads were mapped to the *M. brandtii* (a male sample) genome assembly using BWA-MEM algorithm of BWA 0.7.15 version [30] with–M option. The reads were realigned using the GATK (version 2.5–2) RealignerTargetCreator and IndelRealigner algorithms to minimize the read mismatches [32]. The rmdup command of SAMtools (ver 0.1.19) was used to remove PCR duplicates [31]. Variants were called using mpileup command of SAMtools with–E, -q 20, -A, and–Q 30 options [31]. The called variants were filtered using vcfutils.pl varFilter command of SAMtools (ver 0.1.19) with -d 8 and -D 250 options [31]. To identify X-chromosomal scaffolds from the *M. brandtii* genome assembly, we conducted BLASTn (Blast 2.2.26) with an E-value cutoff of 1E-6 using X-chromosomal CDS sequences of human as queries [39]. Scaffolds having greater than or equal to 10 top hits were considered as X-chromosomal scaffolds.

Comparative evolutionary analysis

Orthologous gene families between *M. rufoniger*'s sequence and 13 mammalian genomes (Seven bat genomes: *M. brandtii*, *M. lucifugus*, *M. davidii*, *E. fuscus*, *P. alecto*, *P. vampyrus*, and *R. aegyptiacus*, and six other mammals: *H. sapiens*, *M. musculus*, *B. taurus*, *E. caballus*, *H. glaber*, and *M. domestica;* S2 Table) were identified using OrthoMCL software (version 2.0.9) by matching and adding the *M. rufoniger* genes to orthologous clusters of *M. brandtii*'s genes, and 6,782 single-copy gene families among the 14 species were collected [7,13]. *M. brandtii*, *M. lucifugus*, *M. davidii*, *E. fuscus*, *P. alecto*, *P. vampyrus*, *R. aegyptiacus*, *H. sapiens*, *M. musculus*, *B. taurus*, *E. caballus*, *H. glaber*, and *M. domestica* genomes and gene sets were downloaded from the NCBI database (S3 Table).

To construct a phylogenetic tree and estimate the divergence time of bats and other mammals, 1,258,141 four-fold degenerate sites from the 6,782 single-copy gene families were used to conduct the multiple sequence alignment (MSA) using MUSCLE (version 3.8.31) program [33]. The phylogenetic tree was constructed among the 14 species using a Randomized Axelerated Maximum Likelihood (RAxML) program (version 8.2) [40]. In RAxML program, GTR gamma model was used as the nucleotide substitution model. In order to check the branch reliability, 1,000 rapid bootstrapping was used. The *M. domestica* was used as an outgroup species. Based on this phylogenetic tree topology, the divergence time was estimated using Reltime-ML in MEGA 7.0 program [34]. In this process, the divergence time at the node between *M. brandtii*–*H. sapiens* was constrained to be 97.5 MYA, and *M. brandtii*–*P. alecto* was constrained to be 62.6 MYA based on the TimeTree database [41].

Amino acid changes were identified by constructing MSAs among the 6,782 single copy gene families using Clustal Omega (version 1.2.4) [42]. Function-altering amino acid changes were predicted using PROVEAN (version 1.1.5) [14]. The MSAs of the *DCT*, *SLC45A2*, *TYRP1*, OCA2, and *N6AMT1* genes were manually checked, and uAACs within misaligned regions were excluded in the variant score analysis. Only homozygous amino acid variants were considered in the amino acid sequence comparison analysis to reduce bias from individual-specific variants.

Demographic history and genetic diversity

The demographic history of the *Myotis* bats was estimated using a pairwise sequential Markovian coalescent (PSMC) program [11]. We mapped the downloaded genome sequencing data of *Myotis* bats to the *M. lucifugus* genome assembly using BWA-MEM algorithm of BWA 0.7.15

version [30] with–M option. The reads were realigned using the GATK (version 2.5–2) RealignerTargetCreator and IndelRealigner algorithms to minimize the read mismatches [32]. The rmdup command of SAMtools (ver 0.1.19) was used to remove PCR duplicates [31]. SAMtools was used to extract diploid genome information from the BAM files [31]. Options of -N25 -t15 -r -p "4+25*2+4+6" were used for the PSMC analysis. The generation time for the *Myotis* bats was estimated as sum of average maturation and gestation time (S16 Table) [43,44]. The mutation rate of *Myotis* bats was estimated by multiplying reported neutral mutation rate for mammals (2.2×10^{-9} per base pair per year) by the generation time (1.2 year) [45]. Atmospheric surface air temperature and global relative sea level data of the past three million years were obtained and used for this analysis [46]. The genomic diversity was calculated by dividing the number of heterozygous SNVs by its genome size (bp) [8]. For the genomic diversity calculation, variants were called using mpileup command of SAMtools with–E, -q 20, -A, and–Q 30 options [31]. The called variants were filtered using vcfutils.pl varFilter command of SAMtools (ver 0.1.19) with -d 8 and -D 250 options [31].

Supporting information

S1 Picture. *M. rufoniger* carcass picture.
(JPG)

S2 Picture. DNA sample electrophoresis.
(JPG)

S1 Fig. Phylogenetic relationship of the *M. rufoniger* sample with other bats. The phylogenetic relationship of *Myotis* bats was inferred from the alignment of mitochondrial cytochrome b coding sequences. The percentage of trees in which the associated taxa clustered together is shown next to the branches. Each node has its species name and GenBank accession number.
(JPG)

S2 Fig. Estimation of genome size using a *K*-mer (17-mers) analysis. The x-axis represents depth, and the y-axis represents proportion, as calculated by the frequency at a given depth divided by the total frequency at all depths.
(PDF)

S3 Fig. Previously reported bats' unique amino acid changes. Previously reported bats' unique amino acid sequence changes within *FSHB*, *GHR*, *IGF1R*, *TP53*, and *MDM2* are highlighted in yellow; (A), Alignment of *FSHB* encoded peptide sequences; (B), Alignment of *GHR*-encoded peptide sequences; (C), Alignment of *IGF1R* encoded peptide sequences; (D), Alignment of *TP53*-encoded peptide sequences; (E), Alignment of *MDM2* encoded peptide sequences; (F), Alignment of *SLC45A2*-encoded peptide sequences; (G), Alignment of *RGS7BP*-encoded peptide sequences; (H), Alignment of *RHO*-encoded peptide sequences; (I), Alignment of *OPN1SW*-encoded peptide sequences; (J), Alignment of *CNGB3*-encoded peptide sequences.
(PDF)

S4 Fig. *Myotis* bats' uAACs within *DCT*, *SLC45A2*, *TYRP1*, and *OCA2* genes. *Myotis* bats' uAACs within *DCT*, *SLC45A2*, *TYRP1*, and *OCA2* genes are highlighted (yellow if PROVEAN score of variant $\leq$ -2.5, unless green). The domain region of human sequences are shaded in gray; (A) Alignment of *DCT* encoded peptide sequences; (B) Alignment of *SLC45A2* encoded peptide sequences; (C) Alignment of *TYRP1* encoded peptide sequences; (D) Alignment of *OCA2* encoded peptide sequences.
(PDF)

S5 Fig. *M. rufoniger* specific amino acid sequence changes. *M. rufoniger* specific amino acid sequence changes within *N6AMT1* gene are highlighted in yellow.
(PDF)

S6 Fig. Sequencing library 574bp QC. (A) Sequencing library 574bp QC; (B) Sequencing library 566bp QC.
(PDF)

S1 Table. Sequencing read filtering result.
(XLSX)

S2 Table. 17-mer statistics information.
(XLSX)

S3 Table. Reference genomes used in this study.
(XLSX)

S4 Table. Base composition of *M. rufoniger* genome. The GC contents were calculated by dividing the number of [(C+G+S)–(M+K+R+Y)] ~ [(C+G+S) + (M+K+R+Y)] by the number of (sum—gap); The proportion of A, C, G, and T, and the proportion of W, S, M, K, and Y were calculated by dividing each number by the number of (sum-gap)
(XLSX)

S5 Table. GC content statistics of *M. rufoniger*.
(XLSX)

S6 Table. Transposon-derived repeats in the *M. rufoniger* genome.
(XLSX)

S7 Table. Comparison of X-chromosomal scaffold heterozygosity.
(XLSX)

S8 Table. *M. rufoniger* unique amino acid changes.
(XLSX)

S9 Table. *M. rufoniger* unique amino acid changes from gap filtered sequences.
(XLSX)

S10 Table. Functional enrichment of *M. rufoniger* uAACs containing genes.
(XLSX)

S11 Table. PROVEAN scores of *DCT*, *SLC45A2*, *TYRP1*, and *OCA2* genes.
(XLSX)

S12 Table. Sum of the PROVEAN scores.
(XLSX)

S13 Table. PROVEAN scores of top 20 ranked genes.
(XLSX)

S14 Table. Sum of the PROVEAN scores of top 20 ranked genes.
(XLSX)

S15 Table. Variants statistics regarding mapping of *Myotis* bat raw reads to the *M. lucifugus* reference.
(XLSX)

S16 Table. Generation time calculation.
(XLSX)

Author Contributions

Conceptualization: YB YSC DYR JB.

Data curation: YB OC S. Jho JHJ HMK.

Formal analysis: YB YJ S. Jeon.

Funding acquisition: JB.

Investigation: YB YJ S. Jeon YC.

Methodology: JB YB.

Project administration: JA DYR JB.

Resources: DYR SL JHK JDL.

Software: YB YJ S. Jeon OC S. Jho JHJ HMK.

Supervision: JB.

Validation: YB CY.

Visualization: YB S. Jeon.

Writing – original draft: JB YB.

Writing – review & editing: YB YJ S. Jeon JA YSC JB.

References

1. Tomes RF, editor ON THE CHARACTERS OF FOUR SPECIES OF BATS INHABITING EUROPE AND ASIA, AND THE DESCRIPTION OF A NEW SPECIES OF VESPERTILIO INHABITING MADAGASCAR. Proceedings of the Zoological Society of London; 1858: Wiley Online Library.

2. Ruedi M, Csorba G, Lin L-K, Chou C-H. Molecular phylogeny and morphological revision of Myotis bats (Chiroptera: Vespertilionidae) from Taiwan and adjacent China. Zootaxa. 2015; 3920(1):301–42.

3. Zhang G, Cowled C, Shi Z, Huang Z, Bishop-Lilly KA, Fang X, et al. Comparative analysis of bat genomes provides insight into the evolution of flight and immunity. Science. 2012:1230835.

4. Seim I, Fang X, Xiong Z, Lobanov AV, Huang Z, Ma S, et al. Genome analysis reveals insights into physiology and longevity of the Brandt's bat Myotis brandtii. Nature communications. 2013; 4.

5. Cho YS, Hu L, Hou H, Lee H, Xu J, Kwon S, et al. The tiger genome and comparative analysis with lion and snow leopard genomes. Nature communications. 2013; 4.

6. Yim H-S, Cho YS, Guang X, Kang SG, Jeong J-Y, Cha S-S, et al. Minke whale genome and aquatic adaptation in cetaceans. Nature genetics. 2014; 46(1):88–92. https://doi.org/10.1038/ng.2835 PMID: 24270359

7. Chung O, Jin S, Cho YS, Lim J, Kim H, Jho S, et al. The first whole genome and transcriptome of the cinereous vulture reveals adaptation in the gastric and immune defense systems and possible convergent evolution between the Old and New World vultures. Genome biology. 2015; 16(1):1.

8. Kim S, Cho YS, Kim H-M, Chung O, Kim H, Jho S, et al. Comparison of carnivore, omnivore, and herbivore mammalian genomes with a new leopard assembly. Genome Biology. 2016; 17(1):211. https://doi.org/10.1186/s13059-016-1071-4 PMID: 27802837

9. Kim YM, Choi EH, Kim SK, Jang KH, Ryu SH, Hwang UW. Complete mitochondrial genome of the Hodgson's bat Myotis formosus (Mammalia, Chiroptera, Vespertilionidae). Mitochondrial DNA. 2011; 22(4):71–3. https://doi.org/10.3109/19401736.2011.624598 PMID: 22040068

10. Miller W, Schuster SC, Welch AJ, Ratan A, Bedoya-Reina OC, Zhao F, et al. Polar and brown bear genomes reveal ancient admixture and demographic footprints of past climate change. Proceedings of the National Academy of Sciences. 2012; 109(36):E2382–E90.

11. Li H, Durbin R. Inference of human population history from individual whole-genome sequences. Nature. 2011; 475(7357):493–6. https://doi.org/10.1038/nature10231 PMID: 21753753

12. Smith JD, Gregory TR. The genome sizes of megabats (Chiroptera: Pteropodidae) are remarkably constrained. Biology letters. 2009; 5(3):347–51. https://doi.org/10.1098/rsbl.2009.0016 PMID: 19324635

13. Li L, Stoeckert CJ, Roos DS. OrthoMCL: identification of ortholog groups for eukaryotic genomes. Genome research. 2003; 13(9):2178–89. https://doi.org/10.1101/gr.1224503 PMID: 12952885

14. Choi Y, Sims GE, Murphy S, Miller JR, Chan AP. Predicting the functional effect of amino acid substitutions and indels. PloS one. 2012; 7(10):e46688. https://doi.org/10.1371/journal.pone.0046688 PMID: 23056405

15. Huang DW, Sherman BT, Lempicki RA. Systematic and integrative analysis of large gene lists using DAVID bioinformatics resources. Nature protocols. 2009; 4(1):44–57. https://doi.org/10.1038/nprot.2008.211 PMID: 19131956

16. Racey P. The prolonged storage and survival of spermatozoa in Chiroptera. Journal of Reproduction and Fertility. 1979; 56(1):391–402. PMID: 381655

17. Hartman CG. On the survival of spermatozoa in the female genital tract of the bat. The Quarterly Review of Biology. 1933; 8(2):185–93.

18. Kitchener D. Reproduction in female Gould's wattled bat, Chalinolobus gouldii (Gray)(Vespertilionidae), in Western Australia. Australian journal of zoology. 1975; 23(1):29–42. PMID: 1140499

19. Sturm RA, Duffy DL. Human pigmentation genes under environmental selection. Genome biology. 2012; 13(9):248. https://doi.org/10.1186/gb-2012-13-9-248 PMID: 23110848

20. Newton J, Cohen-Barak O, Hagiwara N, Gardner JM, Davisson MT, King RA, et al. Mutations in the human orthologue of the mouse underwhite gene (uw) underlie a new form of oculocutaneous albinism, *OCA4*. The American Journal of Human Genetics. 2001; 69(5):981–8. https://doi.org/10.1086/324340 PMID: 11574907

21. Boissy RE, Zhao H, Oetting WS, Austin LM, Wildenberg SC, Boissy YL, et al. Mutation in and lack of expression of tyrosinase-related protein-1 (*TRP-1*) in melanocytes from an individual with brown oculocutaneous albinism: a new subtype of albinism classified as" *OCA3*". American journal of human genetics. 1996; 58(6):1145. PMID: 8651291

22. Manga P, Kromberg J, Box N, Sturm R, Jenkins T, Ramsay M. Rufous oculocutaneous albinism in southern African Blacks is caused by mutations in the *TYRP1* gene. The American Journal of Human Genetics. 1997; 61(5):1095–101. https://doi.org/10.1086/301603 PMID: 9345097

23. Lee S-T, Nicholls RD, Jong MT, Fukai K, Spritz RA. Organization and sequence of the human P gene and identification of a new family of transport proteins. Genomics. 1995; 26(2):354–63. PMID: 7601462

24. Han J, Kraft P, Nan H, Guo Q, Chen C, Qureshi A, et al. A genome-wide association study identifies novel alleles associated with hair color and skin pigmentation. PLoS Genet. 2008; 4(5):e1000074. https://doi.org/10.1371/journal.pgen.1000074 PMID: 18483556

25. Xu X, Dong G-X, Hu X-S, Miao L, Zhang X-L, Zhang D-L, et al. The genetic basis of white tigers. Current biology. 2013; 23(11):1031–5. https://doi.org/10.1016/j.cub.2013.04.054 PMID: 23707431

26. Ren X, Aleshin M, Jo WJ, Dills R, Kalman DA, Vulpe CD, et al. Involvement of N-6 adenine-specific DNA methyltransferase 1 (N6AMT1) in arsenic biomethylation and its role in arsenic-induced toxicity. Environmental health perspectives. 2011; 119(6):771. https://doi.org/10.1289/ehp.1002733 PMID: 21193388

27. Yu HJ, Kang JH, Lee S, Choi YJ, Oh D, Lim JD, et al. Elemental analysis of the liver, kidney, and intestine tissues from a Hodgson's bat (Myotis formosus tsuensis). Korean Journal of Veterinary Research. 2016; 56(1):51–2.

28. Monge G, Jimenez-Espejo FJ, García-Alix A, Martínez-Ruiz F, Mattielli N, Finlayson C, et al. Earliest evidence of pollution by heavy metals in archaeological sites. Scientific reports. 2014; 5:14252–.

29. Patel RK, Jain M. NGS QC Toolkit: a toolkit for quality control of next generation sequencing data. PloS one. 2012; 7(2):e30619. https://doi.org/10.1371/journal.pone.0030619 PMID: 22312429

30. Li H, Durbin R. Fast and accurate short read alignment with Burrows–Wheeler transform. Bioinformatics. 2009; 25(14):1754–60. https://doi.org/10.1093/bioinformatics/btp324 PMID: 19451168

31. Li H, Handsaker B, Wysoker A, Fennell T, Ruan J, Homer N, et al. The sequence alignment/map format and SAMtools. Bioinformatics. 2009; 25(16):2078–9. https://doi.org/10.1093/bioinformatics/btp352 PMID: 19505943

32. McKenna A, Hanna M, Banks E, Sivachenko A, Cibulskis K, Kernytsky A, et al. The Genome Analysis Toolkit: a MapReduce framework for analyzing next-generation DNA sequencing data. Genome research. 2010; 20(9):1297–303. https://doi.org/10.1101/gr.107524.110 PMID: 20644199

33. Edgar RC. MUSCLE: multiple sequence alignment with high accuracy and high throughput. Nucleic acids research. 2004; 32(5):1792–7. https://doi.org/10.1093/nar/gkh340 PMID: 15034147

34. Kumar S, Stecher G, Tamura K. MEGA7: Molecular Evolutionary Genetics Analysis version 7.0 for bigger datasets. Molecular biology and evolution. 2016:msw054.

35. Tamura K, Nei M. Estimation of the number of nucleotide substitutions in the control region of mitochondrial DNA in humans and chimpanzees. Molecular biology and evolution. 1993; 10(3):512–26. PMID: 8336541

36. Felsenstein J. Confidence limits on phylogenies: an approach using the bootstrap. Evolution. 1985:783–91. https://doi.org/10.1111/j.1558-5646.1985.tb00420.x PMID: 28561359

37. Luo R, Liu B, Xie Y, Li Z, Huang W, Yuan J, et al. SOAPdenovo2: an empirically improved memory-efficient short-read de novo assembler. GigaScience. 2012; 1(1):1.

38. Tarailo-Graovac M, Chen N. Using RepeatMasker to identify repetitive elements in genomic sequences. Current Protocols in Bioinformatics. 2009: 4.10. 1–4.

39. Altschul SF, Gish W, Miller W, Myers EW, Lipman DJ. Basic local alignment search tool. Journal of molecular biology. 1990; 215(3):403–10. https://doi.org/10.1016/S0022-2836(05)80360-2 PMID: 2231712

40. Stamatakis A. RAxML version 8: a tool for phylogenetic analysis and post-analysis of large phylogenies. Bioinformatics. 2014; 30(9):1312–3. https://doi.org/10.1093/bioinformatics/btu033 PMID: 24451623

41. Hedges SB, Dudley J, Kumar S. TimeTree: a public knowledge-base of divergence times among organisms. Bioinformatics. 2006; 22(23):2971–2. https://doi.org/10.1093/bioinformatics/btl505 PMID: 17021158

42. Sievers F, Wilm A, Dineen D, Gibson TJ, Karplus K, Li W, et al. Fast, scalable generation of high-quality protein multiple sequence alignments using Clustal Omega. Molecular systems biology. 2011; 7(1):539.

43. Tacutu R, Craig T, Budovsky A, Wuttke D, Lehmann G, Taranukha D, et al. Human ageing genomic resources: integrated databases and tools for the biology and genetics of ageing. Nucleic acids research. 2012:gks1155.

44. Iannelli M. Mathematics of Biology: Lectures given at a Summer School of the Centro Internazionale Matematico Estivo (CIME) held in Cortona (Arezzo), Italy, June 18–30, 1979: Springer Science & Business Media; 2011.

45. Kumar S, Subramanian S. Mutation rates in mammalian genomes. Proceedings of the National Academy of Sciences. 2002; 99(2):803–8.

46. Bintanja R, Van de Wal R. North American ice-sheet dynamics and the onset of 100,000-year glacial cycles. Nature. 2008; 454(7206):869–72. https://doi.org/10.1038/nature07158 PMID: 18704083